

Photopharmacological control of bipolar cells restores visual function in blind mice

Laura Laprell^{1,2#}, Ivan **Tochitsky**³, Kuldeep **Kaur**², Michael B. **Manookin**², Marco **Stein**¹, David M. **Barber**¹, Christian **Schoen**⁴, Stylianos **Michalakis**⁴, Martin **Biel**⁴, Richard H. **Kramer**³, Martin P. **Sumser**¹, Dirk **Trauner**^{1*} and Russell N. **Van Gelder**^{2,5*}

¹ Center of Integrated Protein Science Munich (CIPSM) at the Department of Chemistry Ludwig-Maximilians-Universität München, Munich 81377, Germany

² Department of Ophthalmology, University of Washington School of Medicine, Seattle, WA 98104, USA.

³ Department of Molecular and Cell Biology, University of California, Berkeley, Berkeley, CA 94720, USA

⁴ Center for Integrated Protein Science Munich (CIPSM) at the Department of Pharmacy - Center for Drug Research, Ludwig-Maximilians-Universität München, Munich 81377, Germany

⁵ Department of Biological Structure, University of Washington School of Medicine, Seattle, WA 98104, USA; Department of Pathology, University of Washington School of Medicine, Seattle, WA 98104, USA.

International Max Planck Research School for Molecular and Cellular Life Sciences (IMPRS-LS)

* Corresponding Authors: russvg@uw.edu (Ph: +1 [206 543 7250](tel:2065437250)), dirk.trauner@lmu.de (Ph: +49 89 2180 77714)

Contents

1	SI Figures	S2
2	SI Chemistry.....	S19
2.1	Experimental Procedures for Chemical Synthesis	S19
2.2	Synthesis of DAD and DAD·HCl.....	S21

1 SI Figures

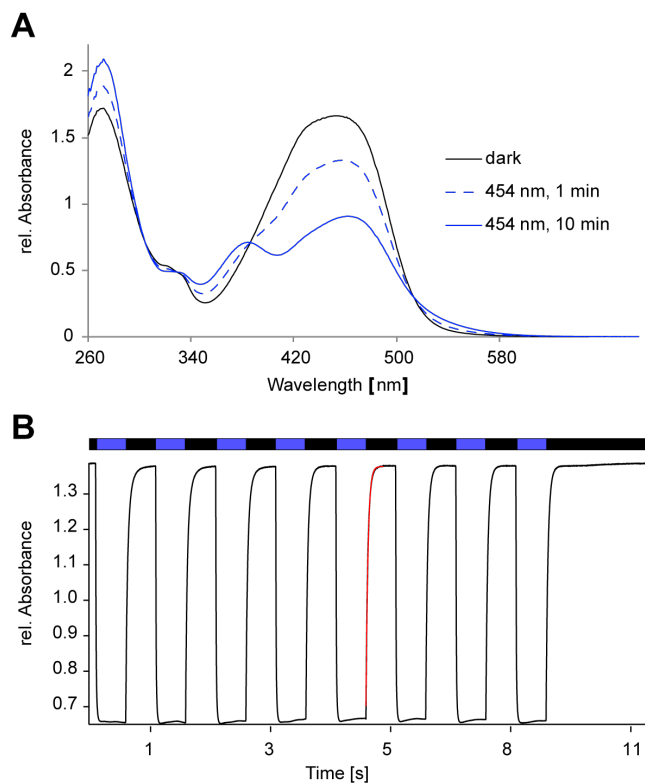


Figure S1 – UV-Vis characterization of DAD. (A) Absorption spectra of dark-adapted *trans*-DAD (black line), *cis*-DAD (blue line). Blue light (454 nm) triggers isomerization of DAD from *cis* to *trans*. **(B)** Kinetics of *trans-cis* and *cis-trans* isomerization determined by UV-Vis spectroscopy at 440 nm. Switching was induced between 460 nm illumination and darkness every 30 seconds. In red: exponential fit of a representative *cis-trans* isomerization ($\tau=33.3$ ms).

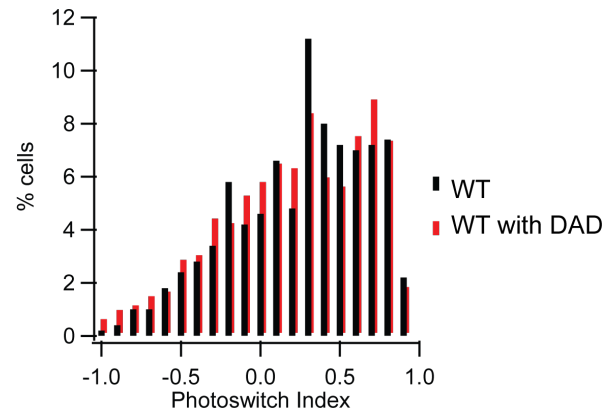


Figure S2 – Effects of DAD on wild type retinas. Photoswitch Index distribution for wild type RGCs before (black) and after treatment (red) with 200 μM DAD (p=0.46).

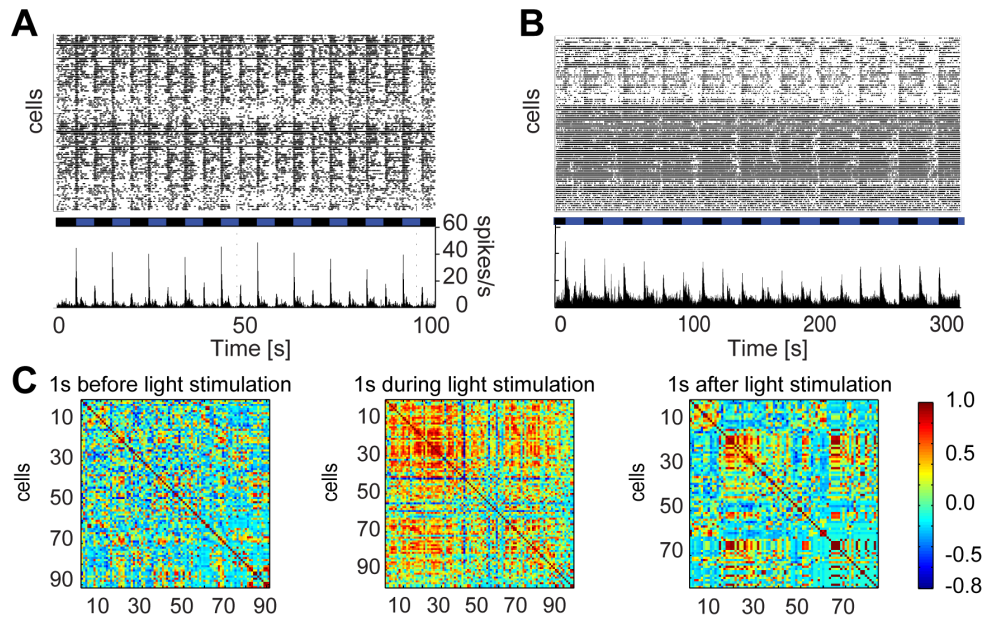


Figure S3 – DAD-treated TKO mouse retinas exhibit light-correlated RGC activity. (A) MEA recording of a DAD-treated TKO retina displaying transient light-off responses in addition to the transient light-on responses. **(B)** Raster plot and histogram of MEA recording in *rd1* retina after treatment with 200 μM DAD. The bar underneath the raster plot indicates light/dark stimulation (blue: 460 nm, black: dark). **(C)** Light response correlation matrices of RGC activity in DAD-treated TKO retina. RGC responses before light stimulation (left), during light stimulation (center) and after switching off light (right). One second binning was applied. Red indicates high correlation while green indicates no correlation. The firing of most RGCs shows a positive correlation during light stimulation (light-ON response) and some RGCs show a positive correlation after light is turned off (light-OFF response).

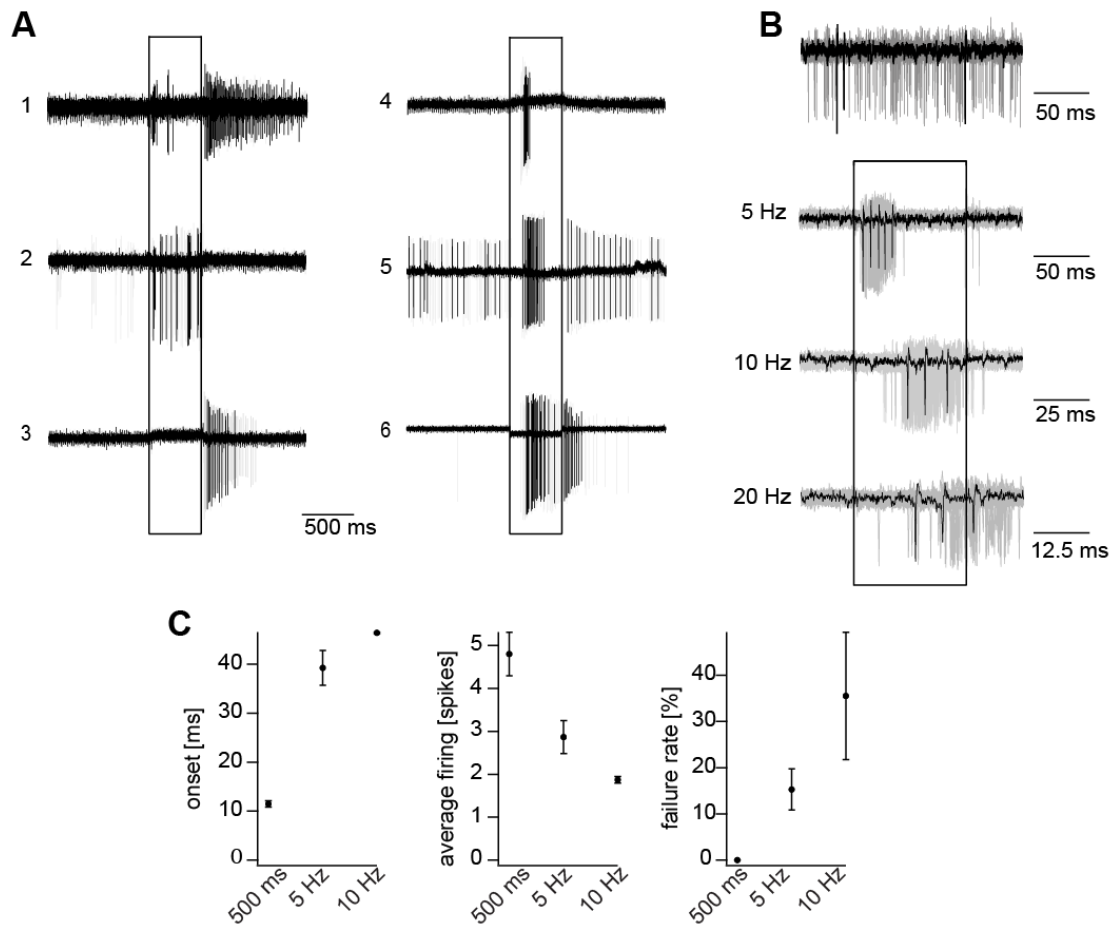


Figure S4. High Frequency stimulation of DAD-treated TKO retinas. (A) Representative traces for RGC on-cell light responses after DAD-treatment. **(B)** Example traces for a high frequency stimulation of a transient light-on RGC. Each recording consists of 100 sweeps. Top: no light stimulation. 5 Hz: 100 ms light, 100 ms dark. 10 Hz: 50 ms light, 50 ms dark. 20 Hz: 25 ms light, 25 ms dark. **(C)** Analysis of high frequency stimulation. Onset in ms after light on. Average firing rate for the period after light was switched on and failure rate (%) based on light stimulation with no spikes in 100 sweeps.

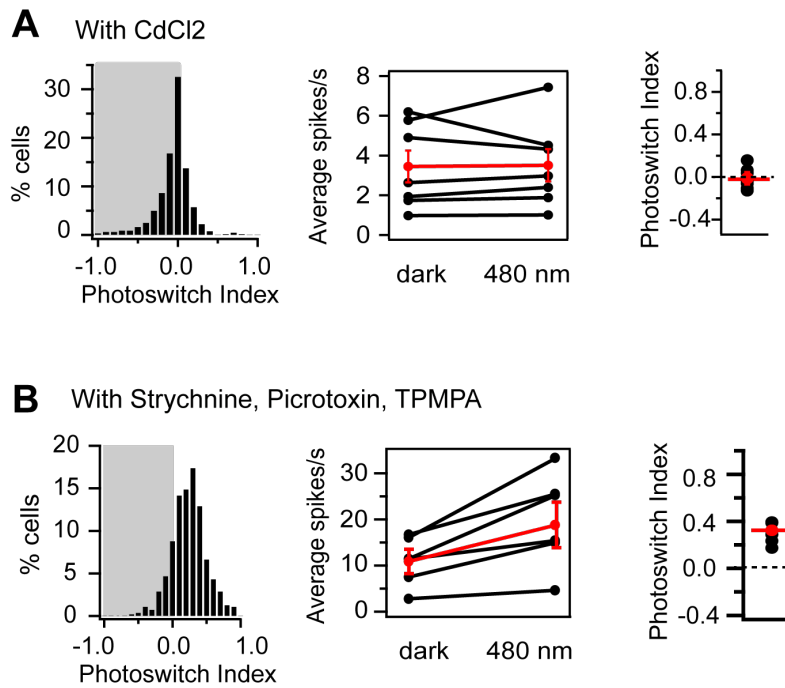


Figure S5 – Pharmacology of DAD. (A) Statistics of light responses in TKO retinas after wash in of CdCl₂. (Left) Distribution of Photoswitch Index values for individual RGCs (n = 688 cells). (Center) Average firing rate in darkness and under 460 nm light (n = 8 retinas). (Right) Average photoswitch index = -0.015 ± 0.094 (n = 8 retinas). **(B)** Statistics of light responses in TKO retinas after wash in of strychnine, picrotoxin and TPMPA. (Left) Distribution of Photoswitch Index values for individual RGCs (n = 882 cells). (Center) Average firing rate in darkness and under 460 nm light (n = 6 retinas). (Right) Average photoswitch index = 0.32 ± 0.030 (n = 6 retinas).

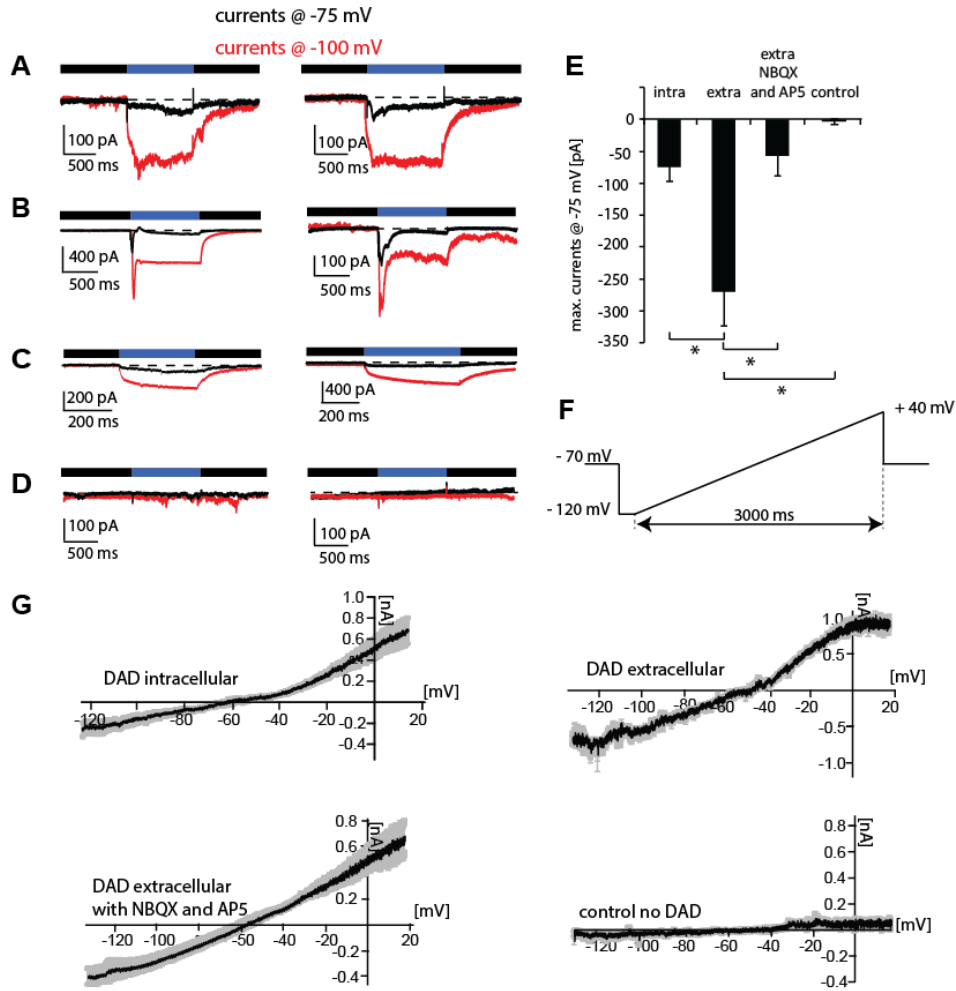


Figure S6 – DAD primarily activates bipolar cells, but also affects HCN channels in RGCs. (A), (B), (C) Representative traces of DAD-mediated photocurrents in retinal ganglion cells, recorded in whole-cell patch clamp mode. Black traces were recorded at a holding potential of -75 mV, red traces at -100 mV. Each trace was averaged from five consecutive sweeps. (A) Intracellular application of DAD (200 μ M) through the patch pipette. (B) Extracellular application of DAD (200 μ M) for 3 minutes. (C) Extracellular DAD in presence of 50 μ M NBQX and D-AP5. (D) Control recordings without DAD application. (E) Quantification of light-induced peak currents at -75 mV: Extracellular DAD ($n=5$), intracellular DAD ($n=7$), extracellular DAD in presence of NBQX and AP5 ($n=4$) and no DAD (control, $n=2$). Statistical analysis was performed using the Student's t-test (Bonferroni corrected $* < 0.02$). (F) IV ramp protocol. (G) Corresponding IV-relationships to (A)-(D). Voltage-ramps were performed between -135 mV and $+20$ mV in darkness and under 460 nm light. Ramps with and without light were subtracted to yield the IV-relationship of light-dependent currents. Average IV are shown as MEAN (black) \pm SE (grey). All experiments were performed in the presence of 1 μ M TTX and corrected for liquid junction potential.

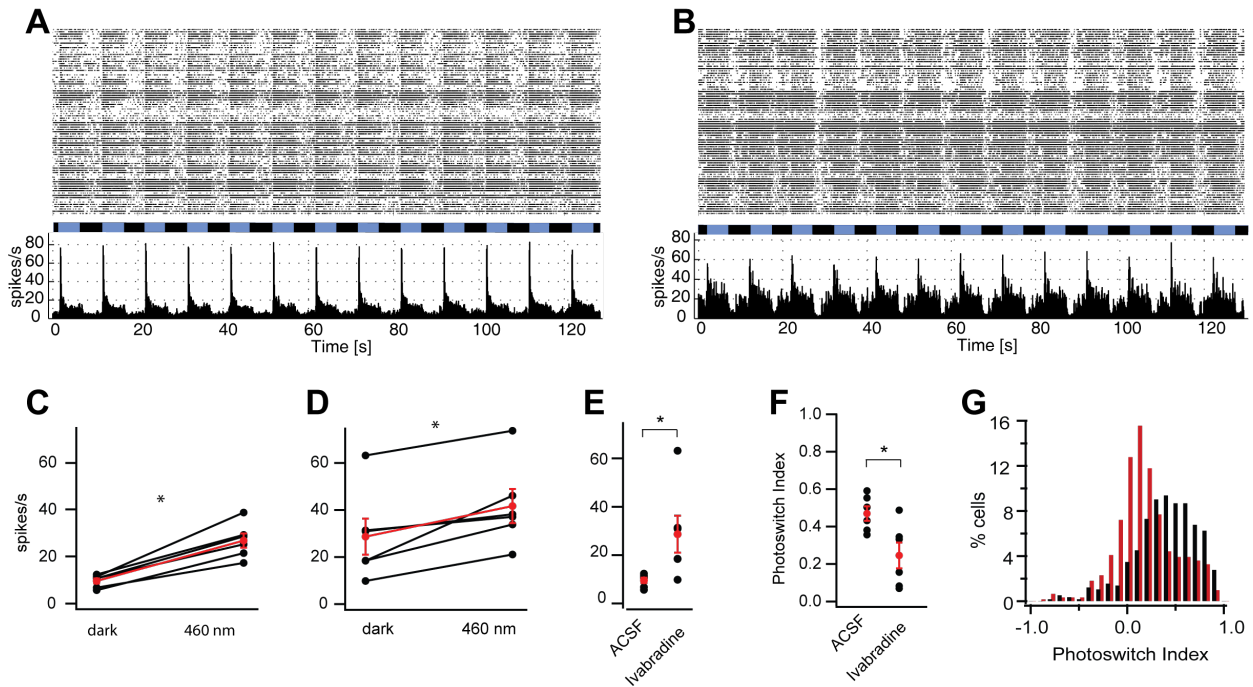


Figure S7 – HCN channel blocker ivabradine does not eliminate DAD-mediated light responses. (A) MEA recording of a DAD-treated TKO retina in ACSF and **(B)** in presence of 75 μ M ivabradine (> 30 min). The bar underneath the raster plot indicates light/dark stimulation (blue: 460 nm, black: dark) **(C)** Statistics of light responses in TKO retinas before and **(D)** after ivabradine application. **(E)** Background activity in darkness in ACSF and ivabradine. **(F)** Photoswitch indices for RGC light-responses in ACSF and ivabradine ($PI_{ACSF} = 0.47 \pm 0.04$ and $PI_{iva} = 0.24 \pm 0.07$, $p = 0.03$). **(G)** Distribution of PIs for RGC populations in ACSF $n = 576$ cells (black) and in presence of ivabradine $n = 615$ cells (red), 6 retinas. Statistical analysis was performed using the Wilcoxon rank sum test.

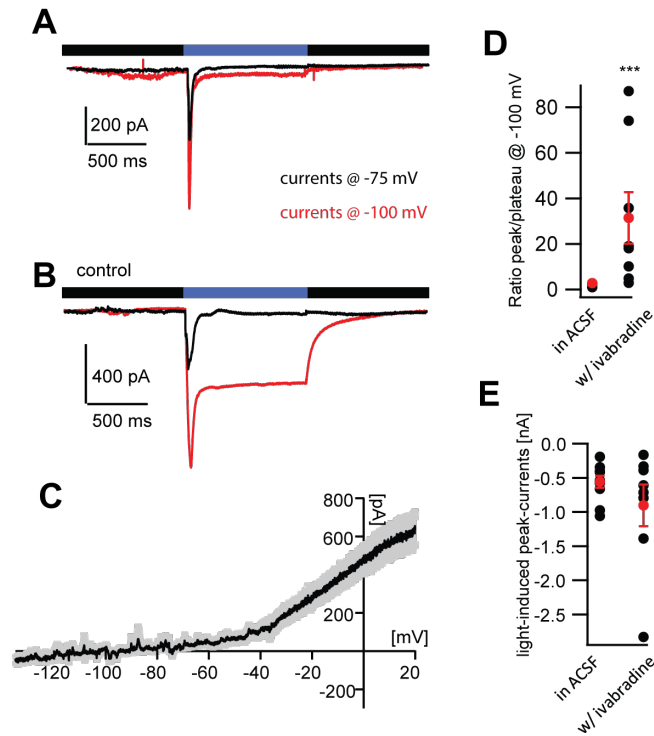


Figure S8 – Effect of HCN channels on DAD-mediated currents in RGCs. (A) Patch clamp recordings at -75 mV (black) and -100 mV (red) in presence of ivabradine and without (B). All traces are peri-stimulus time histogram of 5 consecutive sweeps. (C) IV-relationship of light-induced currents after DAD incubation in presence of 75 μ M ivabradine. (n=6 cells) (D) Ratio of peak currents and plateau currents in absence and presence of ivabradine at -100 mV holding potential. (n=10 and n=8 cells, respectively) ($p = 1.83E-04$) (E) Light-induced peak currents in absence and presence of ivabradine. (n=10 and n=8 cells, respectively) ($p = 0.63$). Statistical analysis was performed using the Wilcoxon rank sum test.

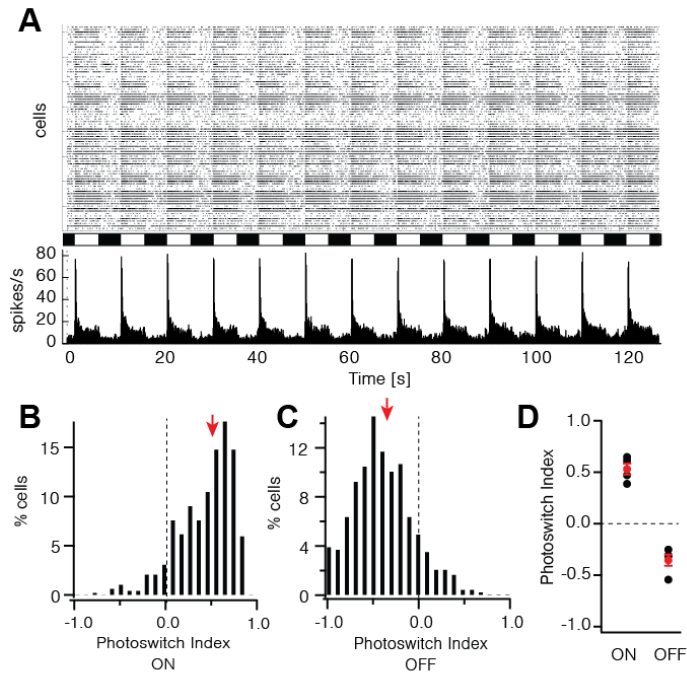


Figure S9 – DAD uptake into retinal cells in presence of 1mM PPADS. (A) Raster plot and histogram of MEA recordings in TKO retina after treatment with 1mM PPADS (>15 min) prior incubation with 200 μ M DAD in 1 mM PPADS (>5 min). The bar underneath the raster plot indicates light/dark stimulation. (B) Distribution of PIs for RGC light-on responses in TKO retinas and (C) for light off-responses (n = 289 cells, 4 retinas). The red arrow indicates the mean PI of the RGC population. (D) Photoswitch index for light on and light off response.

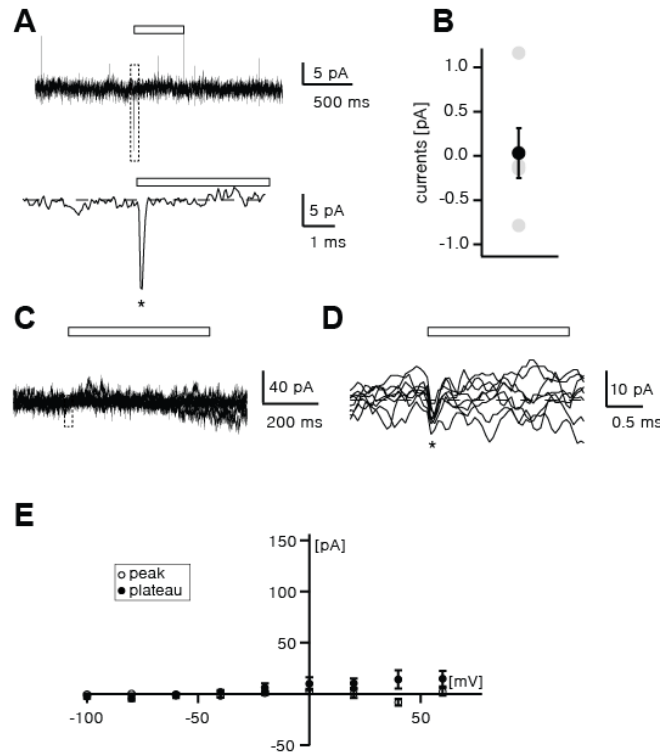


Figure S10 – Control experiments in bipolar cells from TKO mice. (A) Voltage-clamp recording of a bipolar cell before application of DAD. Top: Full trace, peristimulus time histogram (PTSH) of 5 sweeps. Asterisk marks a light artefact induced by the LED. Bottom: Enlargement of dotted box on top. Bar above the trace marks the light stimulation with 460 nm light. **(B)** Peak-currents measured at 0.5 ms (average time to peak for DAD-mediated light responses in bipolar cells (Figure S12B)). **(C)** IV-relationships of in the absence of DAD. **(D)** Enlargement of box in C. **(E)** Analysis of IV-relationships in absence of DAD. (n = 8 cells).

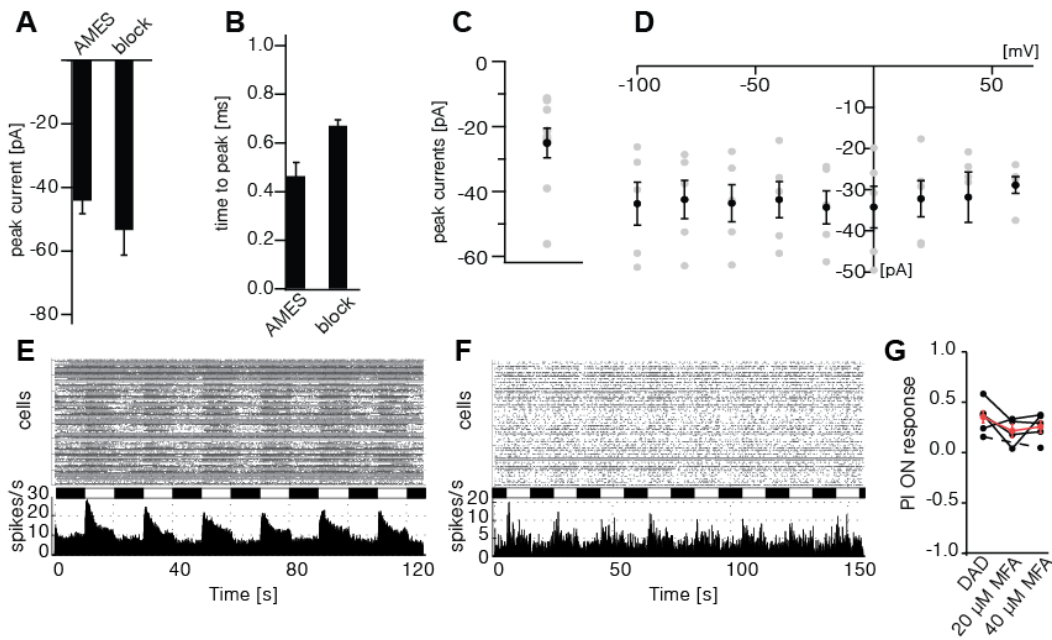


Figure S11. DAD-mediated peak currents in bipolar cell patch clamp experiments. (A) Light induced peak currents in bipolar cells after application of DAD. AMES: no blockers were applied in the extra- and intracellular solution. Block: Application of TTX in the extracellular solution and TEA, Cs⁺ and EGTA in the intracellular solution. **(B)** Time to peak without and with blockers. **(C)** Size of peak currents in bipolar cells after the application of 200 μM MFA to the extracellular solution (wash in for at least 25 min). **(D)** IV-relationship of peak currents after the application of MFA. **(E)** MEA recording after application of 200 μM DAD. **(F)** Same retina as in **(E)** after application of 20 μM MFA (>25 min). **(G)** Photoswitch index of peak firing rate before and after application of 20 μM and 40 μM MFA.

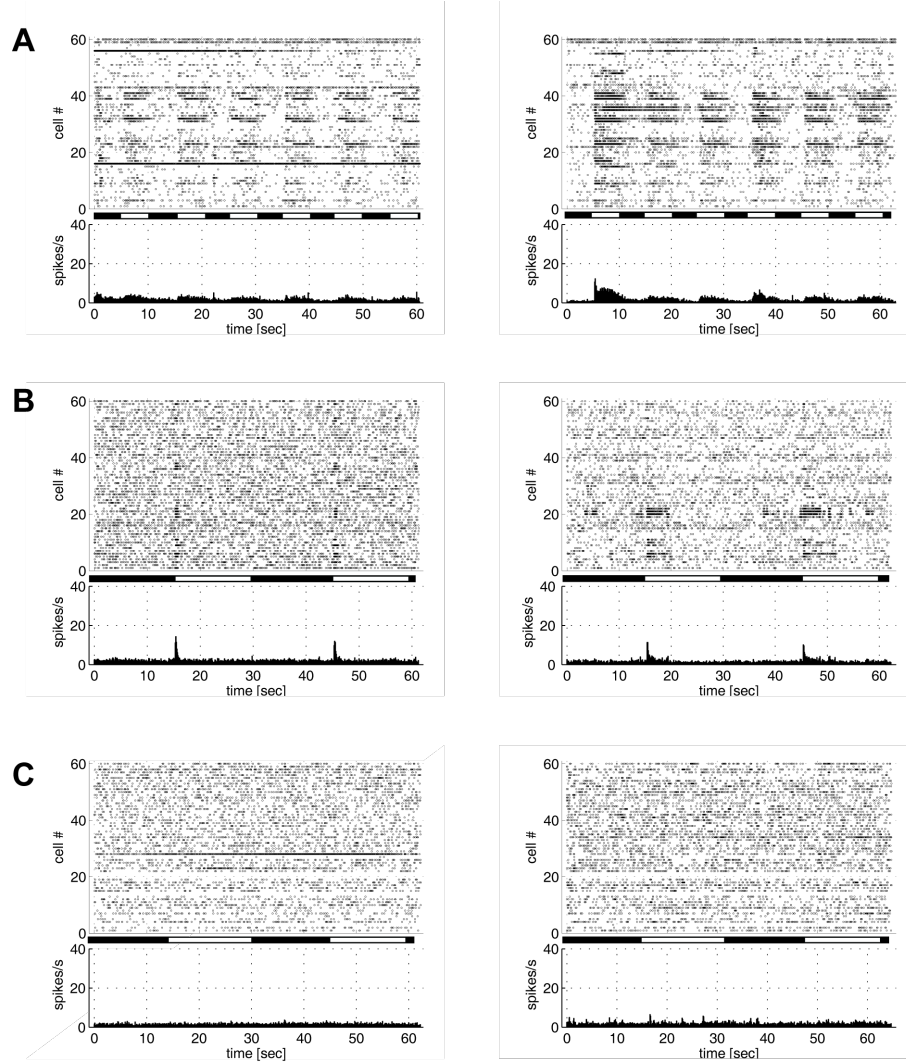


Figure S12 – Representative MEA recordings for non-degenerating retinas before and after application of DAD. (A) WT retina in presence of NBQX and L-AP4 (B) *Gnat1*^{-/-} *Gnat2*^{-/-} *Opn4*^{-/-} retina and (C) *Tra*^{-/-}, *Cnga3*^{-/-}, *Opn4*^{-/-} retinas before (left) and after (right) DAD application.

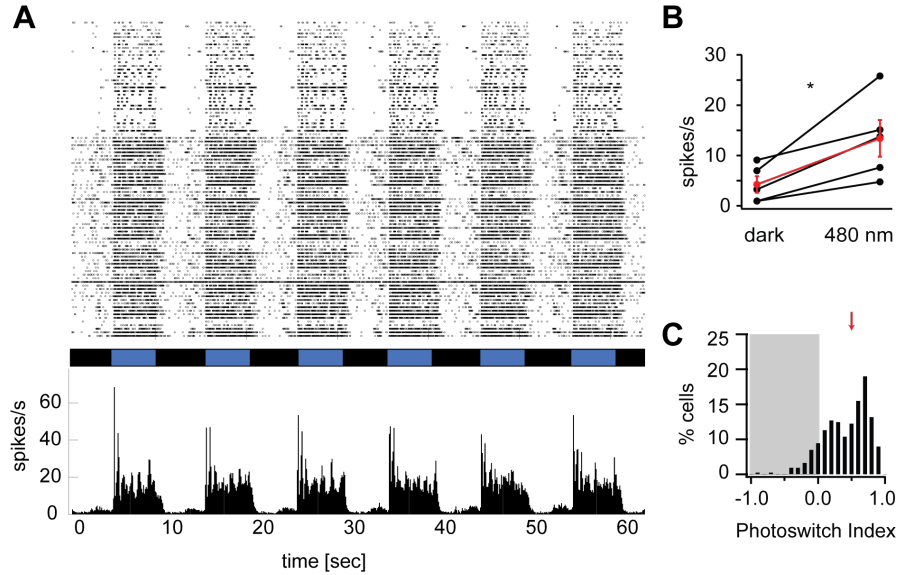


Figure S13 – Block of ON- and OFF-pathways in TKO mice incubated with DAD. (A) MEA recording of a DAD-treated TKO retina in presence of L-AP4 and NBQX. The bar underneath the raster plot indicates light/dark stimulation (blue: 460 nm, black: dark). **(B)** Statistics of light responses. Average spiking rate in darkness and with 460 nm light ($n = 5$ retinas). **(C)** Photoswitch Index distribution for individual RGCs ($n = 439$ RGCs). The red arrow indicates the average $PI = 0.51 \pm 0.11$ ($n = 5$ retinas). Statistical analysis was performed using the signed Wilcoxon rank sum test.

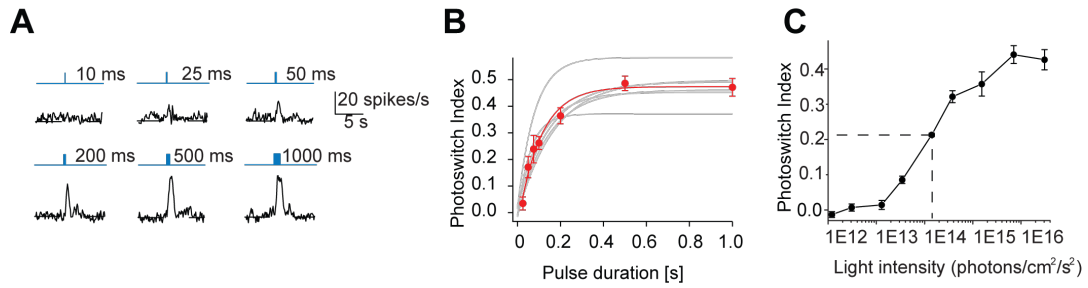


Figure S14 – Light sensitivity of DAD in TKO retinas. (A) Examples for short light-pulse stimulation (intensity = 1.25×10^{16} photons $\text{cm}^{-2} \text{s}^{-1}$, 5.5 mW cm^{-2}). **(B)** Quantification of light-pulse stimulation. 50ms light pulses significantly increase spiking rate above background spiking ($p < 0.05$, $n = 8$ retinas). Grey lines show the monoexponential fit results of individual experiments. Average photoswitch index for different light pulse durations are shown in red. **(C)** Light-intensity versus PI response curve ($n = 5$ retinas). The light intensity threshold for triggering RGC firing was 3×10^{13} photons $\text{cm}^{-2} \text{s}^{-1}$ ($13.5 \mu\text{W cm}^{-2}$) and the maximal light response was achieved with 1×10^{16} photons $\text{cm}^{-2} \text{s}^{-1}$ (4.5 mW cm^{-2}), with a 3 log unit dynamic range.

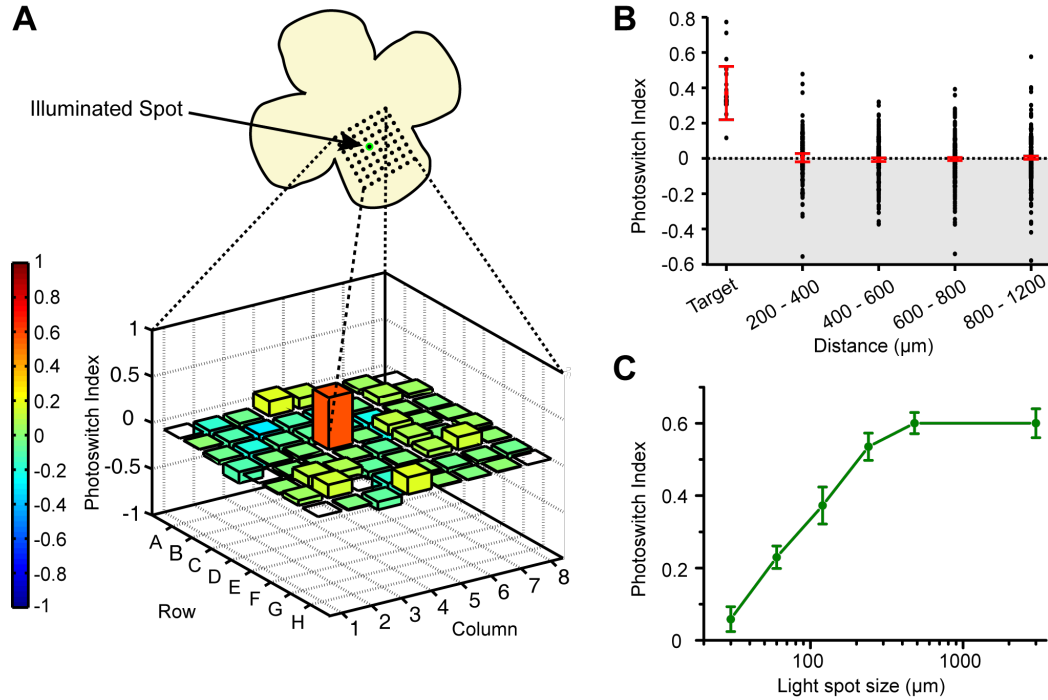


Figure S15 – Small spot stimulation with DAD. (A) Small spot stimulation of a blind retina treated with 200 μM DAD. Illumination was centered on a single electrode (D4) with a diameter of 90 μm . A positive photoswitch index (PI) was only detected from RGCs in the targeted area. **(B)** Quantification of experiment depicted in (A). RGCs in targeted area showed an increase, whereas surrounding RGCs were unaffected (PI = 0.41 ± 0.15 , $n=22$ cells and PI = 0.00 ± 0.11 , $n = 1206$ cells). Single PIs are depicted as black circles as a function of distance from the targeted electrode. Binning of distance 200 μm . Mean \pm 95% confidence intervals are shown in red. **(C)** Receptive field mapping experiment. Light responses of DAD-treated TKO retinas in respect to increasing diameter of light stimulation spots. Saturation of light response is achieved with 240 μm spot size ($n = 16$ cells).

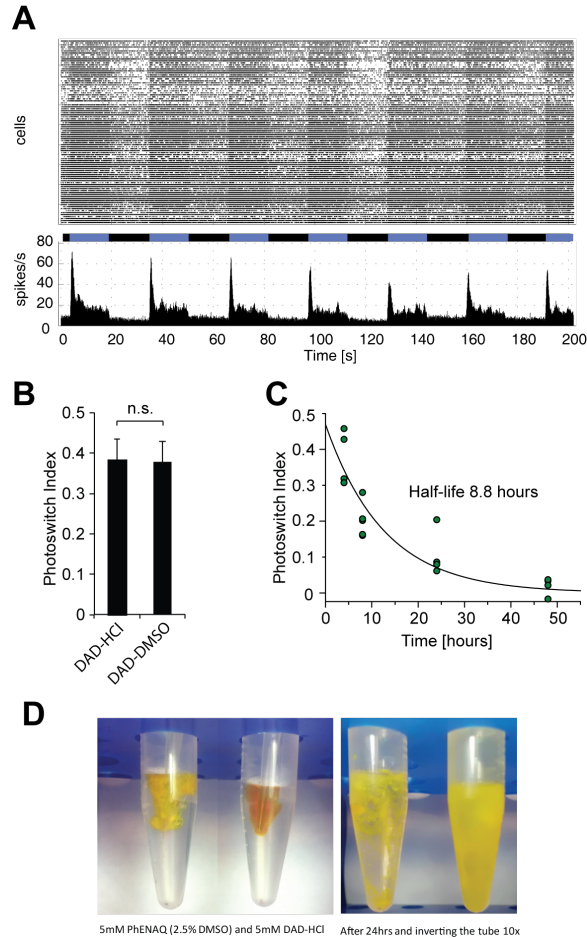


Figure S16 – DAD photosensitizes the *rd1* retina after intravitreal injection. (A) MEA recording from a retina after intravitreal injection of 5 mM DAD after 6 hrs. (B) Comparison of DAD and DAD-HCl after intravitreal injections. After 1 μ L injection of 5mM DAD (0.5 % DMSO) in BSS into *rd1/rd1; Opn4^{-/-}* mice, retinas were dissected after 3 hours ($PI_{D-DMSO} = 0.38 \pm 0.04$, $n = 4$ retinas). Intravitreal injection of 1 μ L DAD-HCl in BSS into *rd1/rd1; Opn4^{-/-}* mice results in a similar photoswitch index after 3 hours ($PI_{D-HCl} = 0.38 \pm 0.05$, $n = 5$ retinas). (C) Persistence of photosensitization after intravitreal injection of 5 mM DAD (half-life = 8.8 hrs). Responses were measured on MEA after dissection of the retinas at several time points after injections. The half-life was calculated by fitting the data with a mono-exponential decay function. (D) Injection of 5 mM PhENAQ (a second generation VGIC blocker, 2.5 % DMSO, left) and 5 mM DAD-HCl in BSS (right) in macaque vitreous. DAD instantly dissolves well in vitreous whereas PhENAQ does not. After 24 hours incubation, DAD-HCl diffused through the whole vitreous solution, while PhENAQ agglutinated.

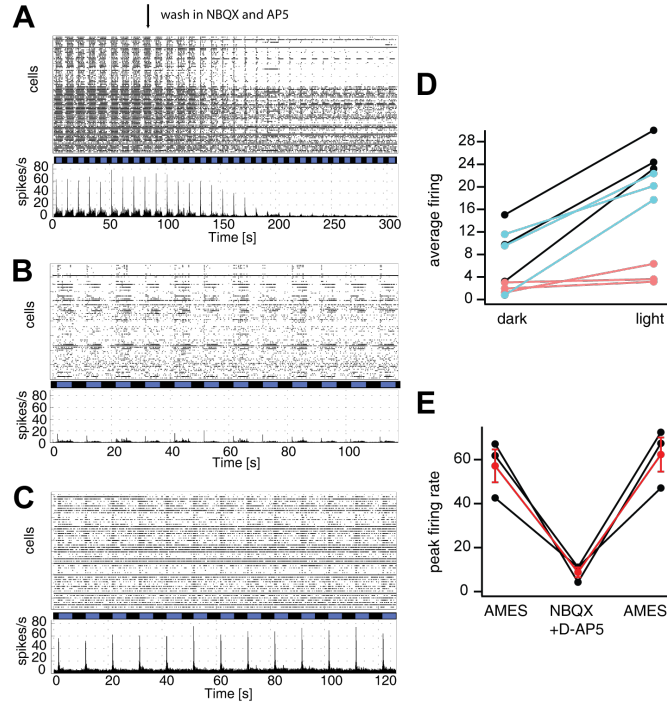


Figure S17 – Long incubation with DAD has only little effect on direct light activation of RGCs. (A) Raster plot and histogram of MEA recording in TKO retina after long (> 20 min) treatment with 200 μ M DAD. The bar underneath the raster plot indicates light/dark stimulation (blue: 460 nm, black: dark). **(B)** MEA recording after wash in of NBQX and AP5. **(C)** MEA recording after subsequent wash out of NBQX and AP5. **(D)** Average firing rates before (black), during NBQX and AP5 treatment (red) and after wash out (blue). **(E)** Analysis of peak firing rate before, during and after NBQX and AP5 treatment (n=3 retinas).

2 SI Chemistry

2.1 Experimental Procedures for Chemical Synthesis

General Experimental Techniques

All reactions were carried out with magnetic stirring using oven-dried glassware under a positive pressure of nitrogen or argon. Syringes used to transfer reagents and solvents were purged with nitrogen or argon prior to use. Low temperature reactions were carried out in a Dewar vessel filled with the appropriate cooling agent e.g. H₂O/ice (0 °C). Reactions using temperatures above room temperature were conducted using a heated oil bath. Yields refer to spectroscopically pure compounds unless otherwise stated.

Solvents and Reagents

Tetrahydrofuran (THF) was distilled under a positive pressure of nitrogen from Na/benzophenone prior to use. Dichloromethane (CH₂Cl₂) and ethanol (EtOH) were purchased from commercial suppliers and used as received. Solvents for extraction and flash column chromatography were purchased in technical grade purity and distilled under reduced pressure prior to use. All other reagents and solvents were purchased from commercial suppliers and used as received.

Chromatography

Reactions and chromatography fractions were monitored by qualitative thin-layer chromatography (TLC) on silica gel F₂₅₄ TLC plates from Merck KGaA. Analytes were visualized by irradiation with UV light and/or by immersion of the TLC plate in aqueous acidic vanillin or potassium permanganate solution followed by heating with a hot-air gun. Flash column chromatography was performed using silica gel, particle size 40–63 μm (eluents are given in parenthesis).

Melting Points

Melting points were measured on an EZ-Melt apparatus from Stanford Research Systems and are uncorrected.

NMR Spectra

NMR spectra were measured on Varian VNMRS 300, VNMRS 400, INOVA 400 or VNMRS 600 instruments operating at 300 MHz, 400 MHz, 400 MHz and 600 MHz for proton nuclei (75 MHz, 100 MHz,

100 MHz and 150 MHz for carbon nuclei) respectively. The ^1H NMR shifts are reported in parts per million (ppm) related to the chemical shift of tetramethylsilane. ^1H NMR shifts were calibrated to the residual solvent resonances: CDCl_3 (7.26 ppm) and CD_3OD (3.31 ppm). ^{13}C NMR shifts were calibrated to the centre of the multiplet signal of the residual solvent resonance: CDCl_3 (77.16 ppm) and CD_3OD (49.00 ppm). ^1H NMR spectroscopic data are reported as follows: Chemical shift in ppm (multiplicity, coupling constants (Hz), integration). The multiplicities are abbreviated as follows: s (singlet), br s (broad singlet), d (doublet), t (triplet), q (quartet) and m (multiplet). Except for multiplets, the chemical shift of all signals is reported as the centre of the resonance range. Additionally to ^1H and ^{13}C NMR measurements, 2D NMR techniques as homonuclear correlation spectroscopy (COSY), heteronuclear single quantum coherence (HSQC) and heteronuclear multiple bond coherence (HMBC) were used to assist signal assignment. All raw fid files were processed and the spectra analyzed using the program MestReNova 9.0 from Mestrelab Research S. L.

Mass Spectra

All high-resolution mass spectra (HRMS) were recorded by the LMU Mass Spectrometry Service. HRMS were recorded on a MAT 90 from Thermo Finnigan GmbH using electrospray ionisation (ESI).

Infrared Spectra

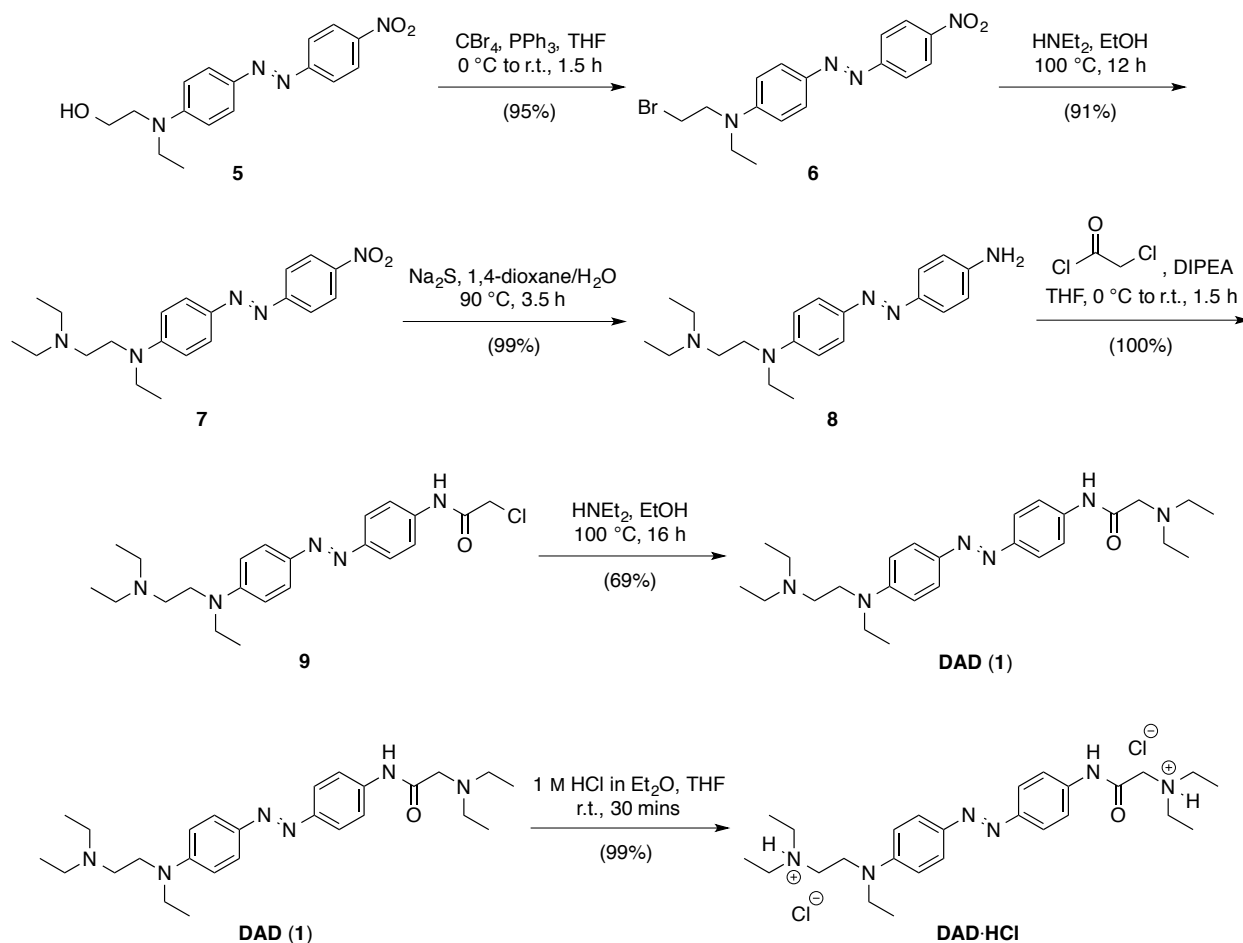
IR spectra were recorded on a PerkinElmer Spectrum BX II FT-IR instrument. The measured wave numbers are reported in cm^{-1} .

UV/Vis Spectra

UV/Vis spectra were recorded on a Varian Cary 50 Scan UV/Vis spectrometer using Helma SUPRASIL precision cuvettes (10 mm light path)

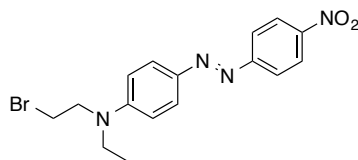
2.2 Synthesis of DAD and DAD·HCl

The synthetic route to **DAD (1)** and **DAD·HCl** is depicted in Scheme 1. The commercially available dye Disperse Red 1 (**5**) was treated with carbon tetrabromide and triphenylphosphine to afford bromide **6** in 95% yield. Nucleophilic substitution of bromide **6** with diethylamine by heating at 100 °C furnished amine **7** in 91% yield. Reduction of the nitro group using sodium sulfide provided aniline **8** in 99% yield. Aniline **8** was then reacted with chloroacetyl chloride yielding chloro amide **9** in quantitative yield. Substitution of the primary chloride with diethylamine at 100 °C furnished **DAD (1)** in 69% yield. Treatment of **DAD (1)** with 1.0 M HCl in Et₂O furnished **DAD·HCl** in 99% yield.



Scheme 1. Synthetic route to **DAD (1)** and **DAD·HCl**.

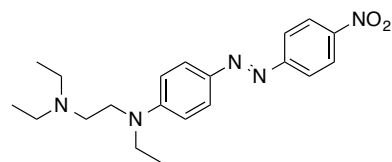
Synthesis and characterization of *N*-(2-bromoethyl)-*N*-ethyl-4-[(*E*)-(4-nitrophenyl)diazenyl] aniline (**6**).



To a stirred solution of Disperse Red 1 (2.00 g, 6.36 mmol, 1.0 equiv.) in THF (40 mL) at 0 °C was added CBr₄ (2.42 g, 7.31 mmol, 1.15 equiv.) and PPh₃ (1.92 g, 7.31 mmol, 1.15 equiv.). The resulting mixture was warmed to r.t. and stirred for 1.5 h. The reaction mixture was concentrated under reduced pressure and the residue was purified by flash column chromatography on silica gel eluting with hexanes/EtOAc (6:1) to afford compound **6** (2.28 g, 95%) as a deep red solid.

mp: 142–143 °C; **TLC** (hexanes/EtOAc, 4:1): *R_f* = 0.60; **¹H NMR** (300 MHz, CDCl₃): δ 8.38–8.29 (m, 2H), 7.98–7.87 (m, 4H), 6.82–6.72 (m, 2H), 3.82 (t, *J* = 7.8 Hz, 2H), 3.62–3.45 (m, 4H), 1.27 (t, *J* = 7.1 Hz, 3H); **¹³C NMR** (75 MHz, CDCl₃): δ 156.8, 150.6, 147.7, 144.3, 126.4, 124.8, 122.9, 111.6, 52.5, 45.9, 27.8, 12.8; **IR** (neat): 2974, 1601, 1559, 1516, 1465, 1424, 1406, 1390, 1354, 1340, 1311, 1271, 1254, 1218, 1202, 1155, 1141, 1106, 1077, 1002, 858, 823, 756, 724, 686, 668 cm⁻¹; **HRMS** (*m/z*): [(*M*+*H*)⁺] calcd. for C₁₆H₁₈BrN₄O₂⁺, 377.0608; found 377.0610.

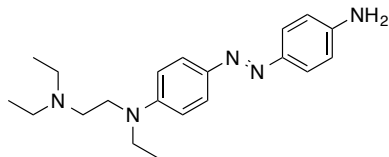
Synthesis and characterization of *N,N,N'*-triethyl-*N'*-{4-[(*E*)-(4-nitrophenyl)diazenyl]phenyl}ethane-1,2-diamine (**7**).



In a pressure tube containing a stirred solution of compound **6** (300 mg, 0.800 mmol, 1.0 equiv.) in EtOH (4.0 mL) at r.t. was added diethylamine (0.83 mL, 8.00 mmol, 10.0 equiv.). The pressure tube was sealed and the resulting mixture was heated to 100 °C for 12 h. The reaction mixture was cooled to r.t. and then concentrated under reduced pressure. Purification by flash column chromatography on silica gel eluting with CH₂Cl₂/MeOH (100:0 → 2:1) afforded compound **7** (268 mg, 91%) as a deep red oil.

TLC (CH₂Cl₂/MeOH, 20:1): *R_f* = 0.30; **¹H NMR** (400 MHz, CDCl₃): δ 8.35–8.30 (m, 2H), 7.94–7.87 (m, 4H), 6.78–6.73 (m, 2H), 3.55–3.49 (m, 4H), 2.70–2.63 (m, 2H), 2.61 (q, *J* = 7.2 Hz, 4H), 1.26 (t, *J* = 7.1 Hz, 3H), 1.07 (t, *J* = 7.2 Hz, 6H); **¹³C NMR** (100 MHz, CDCl₃): δ 157.1, 151.6, 147.4, 143.6, 126.5, 124.8, 122.7, 111.3, 50.6, 49.9, 47.8, 46.1, 12.6, 12.2; **IR** (neat): 2969, 1602, 1557, 1513, 1470, 1423, 1407, 1390, 1340, 1255, 1201, 1156, 1142, 1105, 1072, 998, 859, 824, 755, 721, 687, 666 cm⁻¹; **HRMS** (*m/z*): [(*M*+*H*)⁺] calcd. for C₂₀H₂₈N₅O₂⁺, 370.2238; found 370.2238.

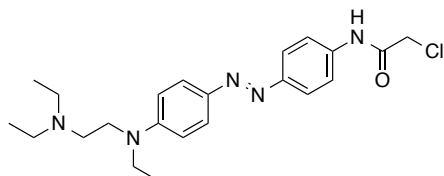
Synthesis and characterization of *N*-{4-[(*E*)-(4-aminophenyl)diazenyl]phenyl}-*N,N'*-triethylethane-1,2-diamine (8**).**



To a stirred solution of compound **7** (288 mg, 0.780 mmol, 1.0 equiv.) in 1,4-dioxane (12.0 mL) and H₂O (1.0 mL) at r.t. was added Na₂S (106 mg, 1.36 mmol, 1.7 equiv.). The resulting mixture was heated to 90 °C for 2 h. After this time, TLC analysis indicated that the starting material had not been consumed. A second portion of Na₂S (53 mg, 0.680 mmol, 0.9 equiv.) was added and the reaction mixture was heated to 90 °C for a further 1.5 h. The reaction was quenched with sat. aq. NaHCO₃ (30 mL) and extracted with CH₂Cl₂ (3 × 20 mL). The combined organic extracts were washed with brine (50 mL), dried over MgSO₄, filtered and concentrated under reduced pressure. Purification by flash column chromatography on silica gel eluting with CH₂Cl₂/MeOH (20:1 → 10:1) afforded compound **8** (260 mg, 99%) as a deep red oil.

TLC (CH₂Cl₂/MeOH, 10:1): R_f = 0.30; **¹H NMR** (300 MHz, CDCl₃): δ 7.83–7.74 (m, 2H), 7.75–7.68 (m, 2H), 6.77–6.67 (m, 4H), 3.90 (br s, 2H), 3.58–3.39 (m, 4H), 2.73–2.55 (m, 6H), 1.21 (t, *J* = 7.1 Hz, 3H), 1.08 (t, *J* = 7.8 Hz, 6H); **¹³C NMR** (75 MHz, CDCl₃): δ 149.4, 148.2, 146.2, 143.6, 124.6, 124.2, 115.0, 111.3, 50.4, 49.4, 47.7, 45.8, 12.6, 11.9; **IR** (neat): 3337, 3209, 2968, 2932, 2811, 1619, 1591, 1561, 1511, 1468, 1450, 1395, 1350, 1294, 1276, 1245, 1201, 1149, 1071, 998, 944, 834, 821, 730 cm⁻¹; **HRMS** (*m/z*): [(M+H)⁺] calcd. for C₂₀H₃₀N₅⁺, 340.2496; found 340.2497.

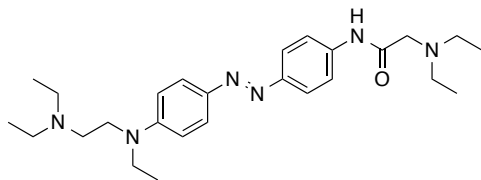
Synthesis and characterization of 2-chloro-*N*-{4-[(*E*)-(4-{[2-(diethylamino)ethyl](ethyl)amino}phenyl)diazenyl]phenyl}acetamide (9**).**



To a stirred solution of compound **8** (181 mg, 0.530 mmol, 1.0 equiv.) in THF (25 mL) at 0 °C was added DIPEA (0.11 mL, 0.640 mmol, 1.2 equiv.) and chloroacetyl chloride (64 μL, 0.800 mmol, 1.5 equiv.). The resulting mixture was allowed to warm to r.t. and stirred for 1.5 h. The reaction mixture was concentrated under reduced pressure and the residue was purified by flash column chromatography on silica gel eluting with CH₂Cl₂/MeOH (15:1 → 10:1) to afford compound **9** (226 mg, 100%) as a deep red oil.

TLC (CH₂Cl₂/MeOH, 10:1): R_f = 0.34; **¹H NMR** (400 MHz, CDCl₃): δ 8.33 (br s, 1H), 7.89–7.81 (m, 4H), 7.70–7.66 (m, 2H), 6.76–6.72 (m, 2H), 4.22 (s, 2H), 3.56–3.45 (m, 4H), 2.73–2.57 (m, 6H), 1.23 (t, *J* = 7.1 Hz, 3H), 1.08 (t, *J* = 7.1 Hz, 6H); **¹³C NMR** (100 MHz, CDCl₃): δ 163.8, 150.5, 150.3, 143.4, 137.6, 125.4, 123.3, 120.3, 111.2, 50.4, 49.6, 47.8, 45.9, 43.1, 12.6, 12.0; **IR** (neat): 3249, 2969, 2810, 1675, 1596, 1541, 1514, 1446, 1422, 1393, 1350, 1313, 1276, 1248, 1198, 1154, 1139, 1073, 998, 844, 821, 731, 696 cm⁻¹; **HRMS** (*m/z*): [(M+H)⁺] calcd. for C₂₂H₃₁ClN₅O⁺, 416.2212; found 416.2215.

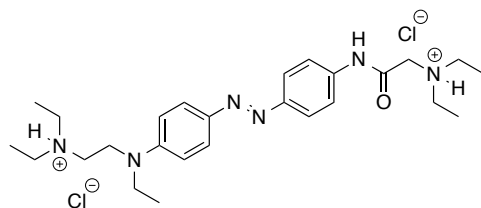
Synthesis and characterization of *N*²-(aminomethyl)-*N*-{4-[(*E*)-(4-{[2-(diethylamino)ethyl](ethyl)amino}phenyl)diazenyl]phenyl}-*N*²-ethylglycinamide (DAD** (**1**)).**



In a pressure tube containing a stirred solution of compound **9** (218 mg, 0.520 mmol, 1.0 equiv.) in EtOH (5 mL) at r.t. was added diethylamine (0.54 mL, 5.20 mmol, 10.0 equiv.). The pressure tube was sealed and the resulting mixture was heated to 100 °C for 16 h. The reaction mixture was cooled to r.t. and concentrated under reduced pressure. Purification by column chromatography on silica gel eluting with CH₂Cl₂/MeOH (30:1 → 25:1) afforded **DAD** (**1**) (161 mg, 69%) as a deep red oil.

TLC (CH₂Cl₂/MeOH, 10:1): R_f = 0.41; **¹H NMR** (600 MHz, CDCl₃): δ 9.54 (br s, 1H), 7.87–7.80 (m, 4H), 7.71–7.66 (m, 2H), 6.76–6.69 (m, 2H), 3.54–3.44 (m, 4H), 3.17 (s, 2H), 2.69–2.63 (m, 6H), 2.61 (q, *J* = 7.0 Hz, 4H), 1.22 (t, *J* = 7.1 Hz, 3H), 1.11 (t, *J* = 7.2 Hz, 6H), 1.07 (t, *J* = 7.1 Hz, 6H); **¹³C NMR** (150 MHz, CDCl₃): δ 170.3, 150.1, 149.7, 143.4, 138.8, 125.2, 123.3, 119.5, 111.2, 58.3, 50.4, 49.6, 49.0, 47.8, 45.8, 12.6, 12.6, 12.1; **IR** (neat): 3276, 2967, 2932, 2813, 1692, 1597, 1560, 1510, 1447, 1420, 1393, 1350, 1299, 1276, 1247, 1202, 1152, 1139, 1070, 998, 905, 845, 820, 730, 668 cm⁻¹; **HRMS** (*m/z*): [(*M*+*H*)⁺] calcd. for C₂₆H₄₁N₆O⁺, 453.3336; found 453.3337; **UV/Vis**: λ_{max} = 454 nm (50 μM in DMSO), λ_{max} = 450 nm (50 μM in PBS buffer).

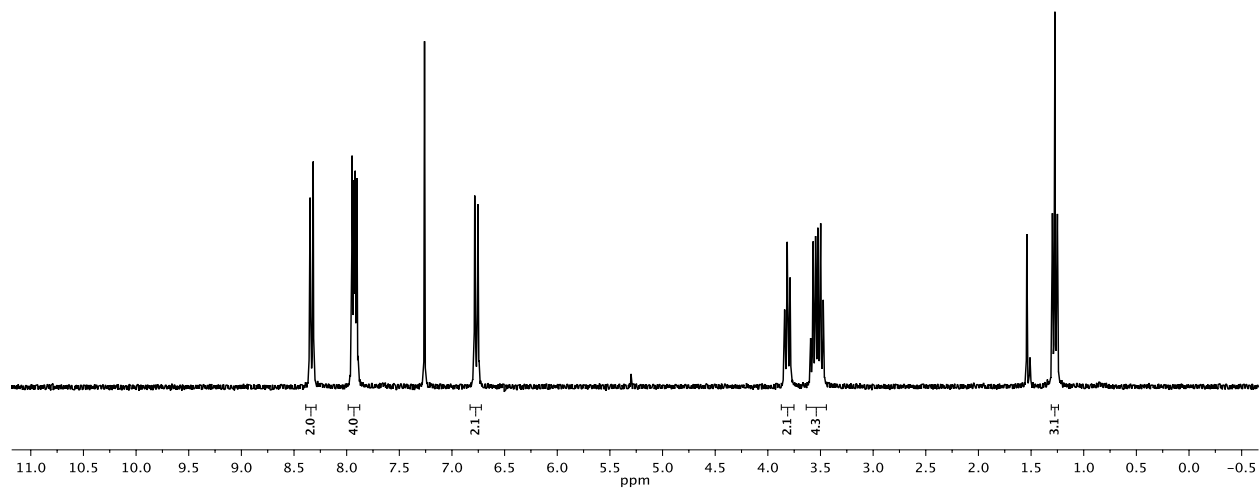
Synthesis and characterization of *N*²-(aminomethyl)-*N*-{4-[(*E*)-(4-{[2-(diethylamino)ethyl](ethyl)amino}phenyl)diazenyl]phenyl}-*N*²-ethylglycinamide dihydrochloride (DAD·HCl**).**



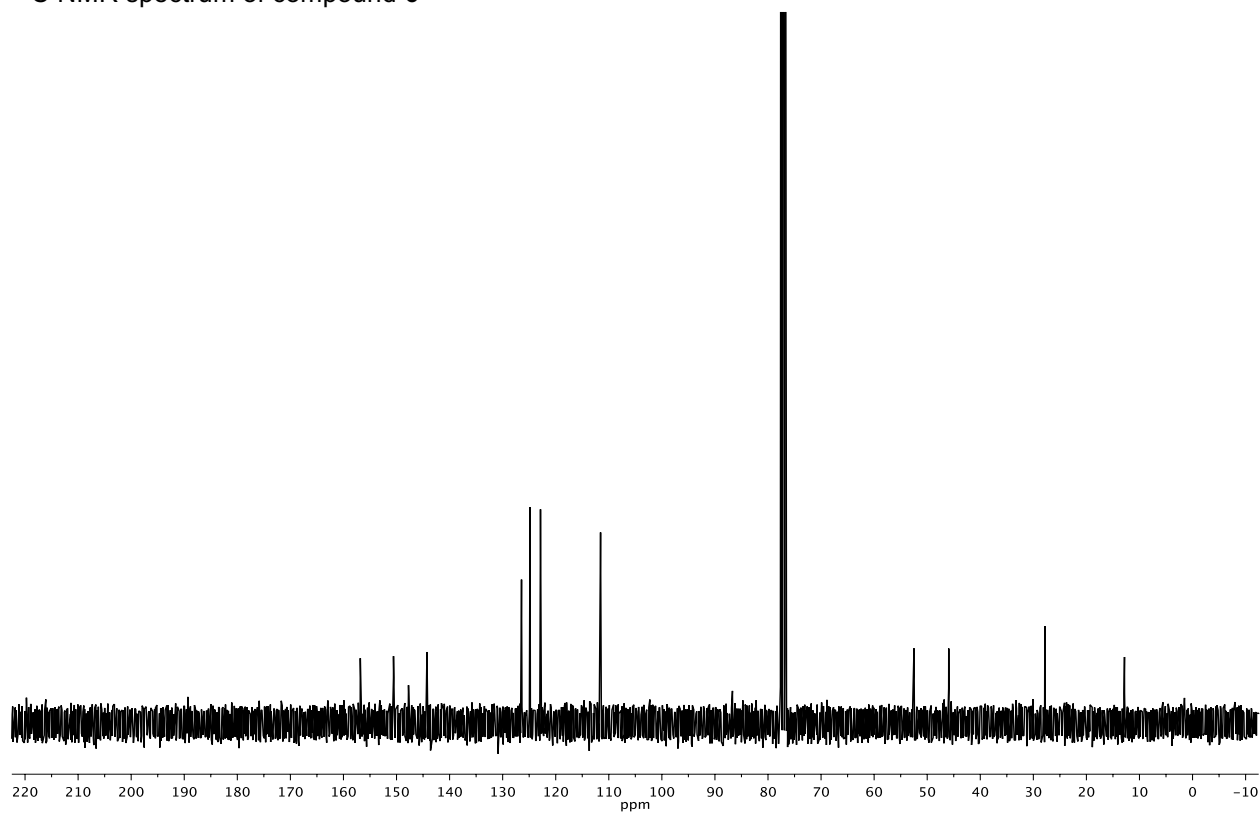
To a stirred solution of **DAD** (**1**) (226 mg, 0.500 mmol, 1.0 equiv.) in THF/Et₂O (1:1, 4.0 mL) at r.t. was added a solution of HCl (2.0 mL, 1.0 M in Et₂O, 4.0 equiv.). The resulting mixture was stirred at r.t. for 30 min. The reaction mixture was concentrated under reduced pressure and the residue was dissolved in MeOH. Concentration under reduced pressure afforded **DAD·HCl** (261 mg, 99%) as a dark purple amorphous solid.

mp: 76–79 °C; **¹H NMR** (400 MHz, CD₃OD): δ 8.01–7.90 (m, 2H), 7.81–7.70 (m, 4H), 7.21–7.08 (m, 2H), 4.19 (s, 2H), 4.12–3.99 (m, 2H), 3.73–3.60 (m, 2H), 3.42–3.16 (m, 10H), 1.32 (t, *J* = 7.2 Hz, 12H), 1.22 (t, *J* = 6.9 Hz, 3H); **¹³C NMR** (100 MHz, CD₃OD): δ 164.5, 154.9 (br s), 143.7, 141.6 (br s), 140.5, 131.0 (br s), 122.3, 121.6, 116.3 (br s), 55.1, 50.8, 49.4, 48.7, 48.4, 47.1, 12.8, 9.6, 9.2; **IR** (neat): 3852, 3837, 3820, 3744, 3734, 3647, 3628, 3437, 2972, 2642, 1734, 1717, 1700, 1684, 1652, 1635, 1597, 1558, 1507, 1456, 1394, 1250, 1140, 668 cm⁻¹; **HRMS** (*m/z*): [(*M*-2HCl+*H*)⁺] calcd. for C₂₆H₄₁N₆O⁺, 453.3336; found 453.3333; **UV/Vis**: λ_{max} = 425 nm (50 μM in DMSO), λ_{max} = 445 nm (50 μM in PBS buffer).

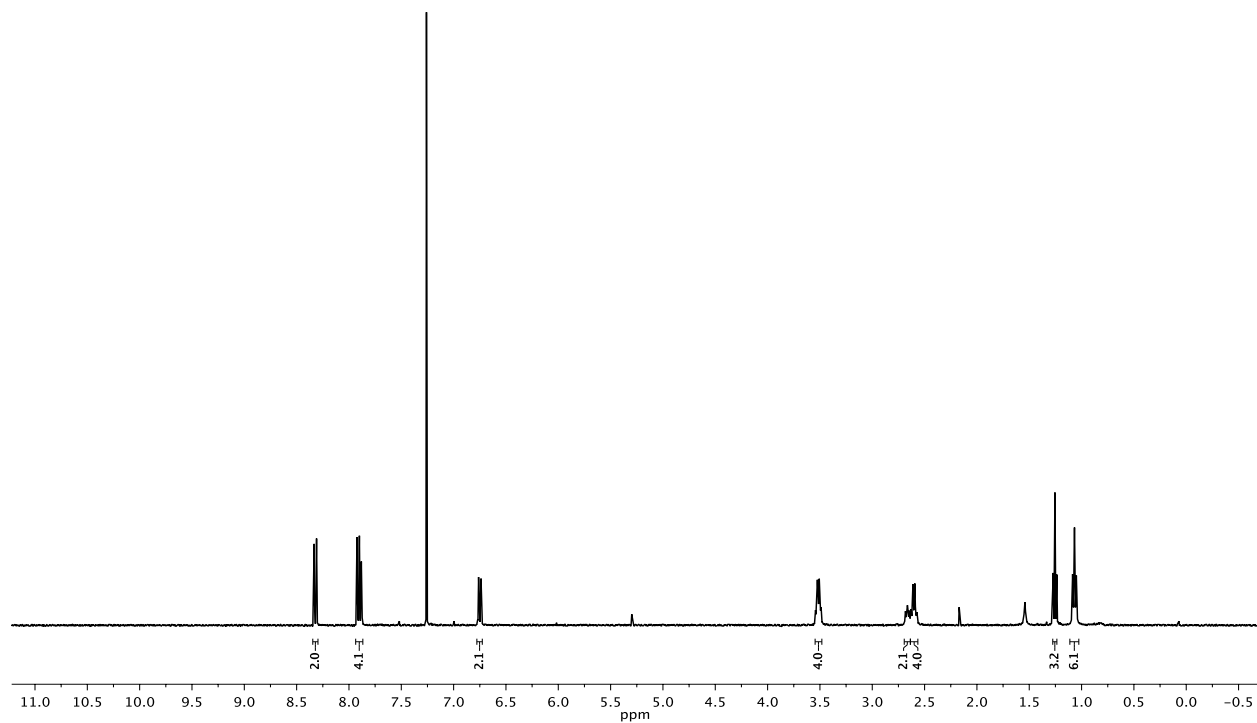
^1H NMR spectrum of compound **6**



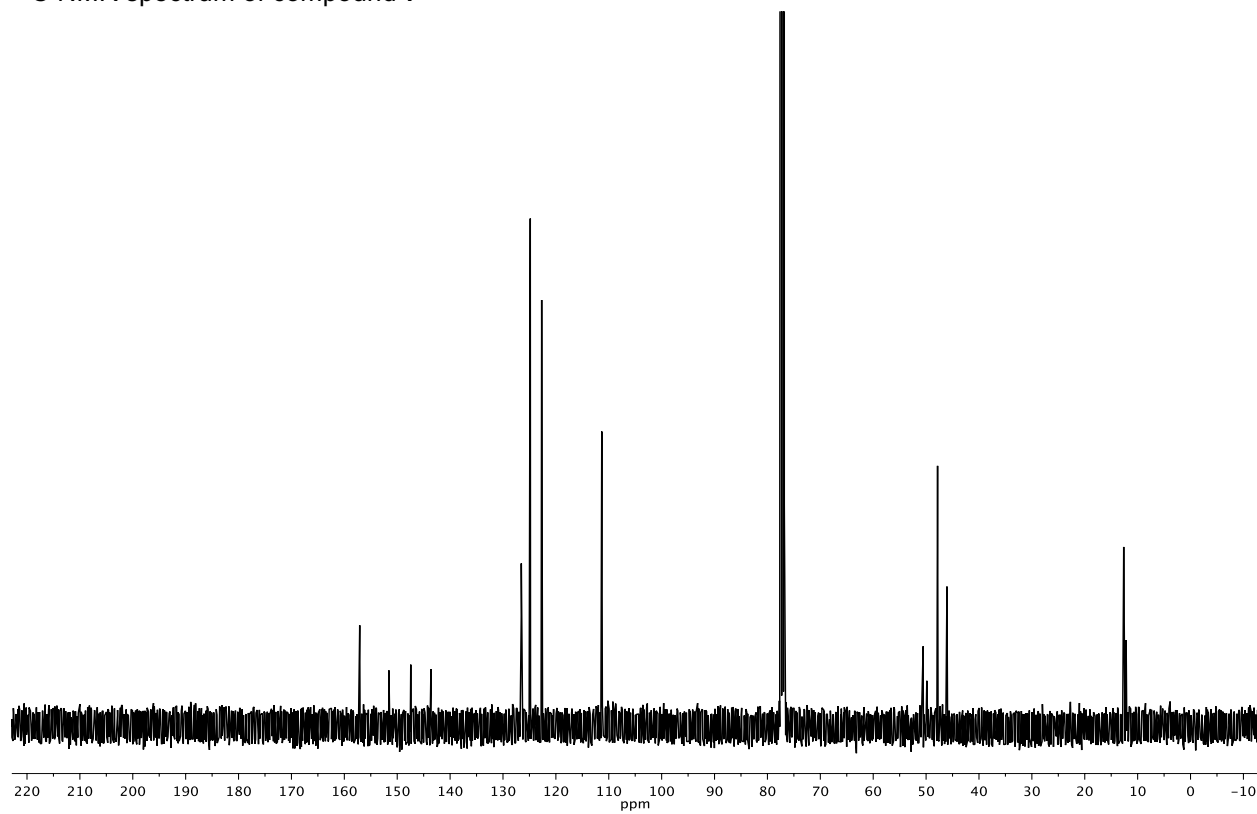
^{13}C NMR spectrum of compound **6**



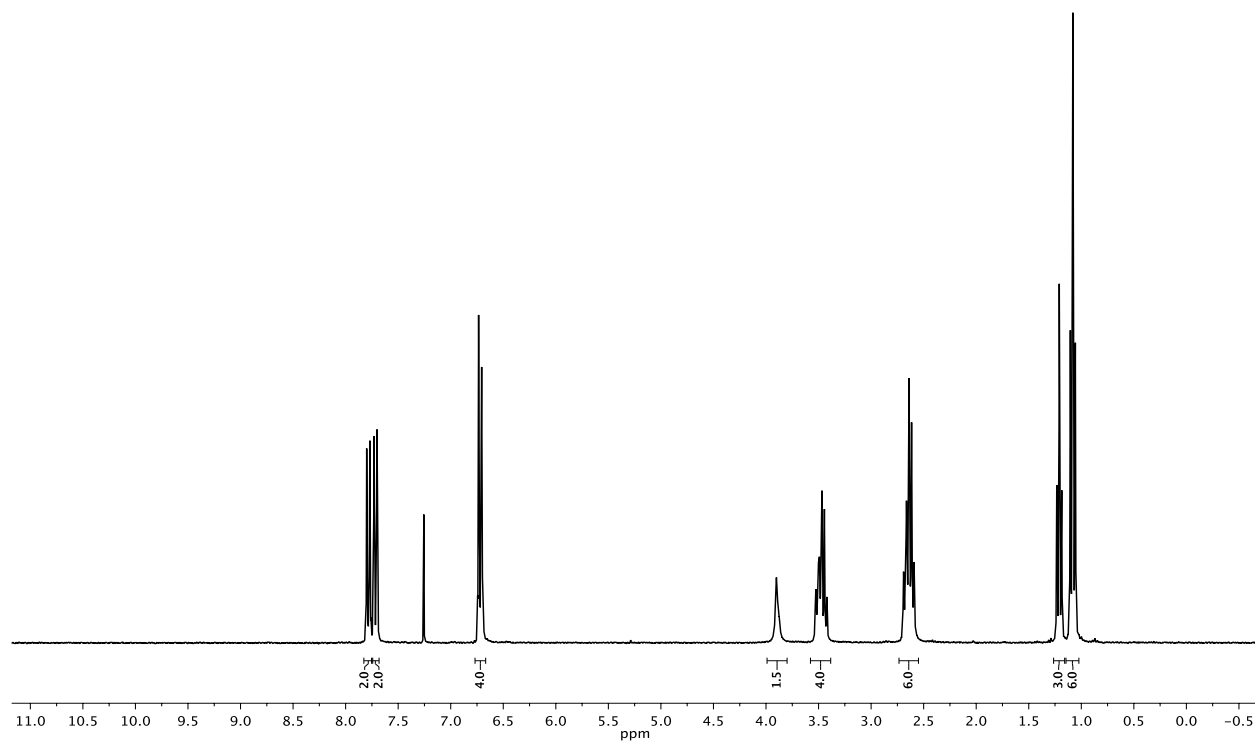
^1H NMR spectrum of compound 7



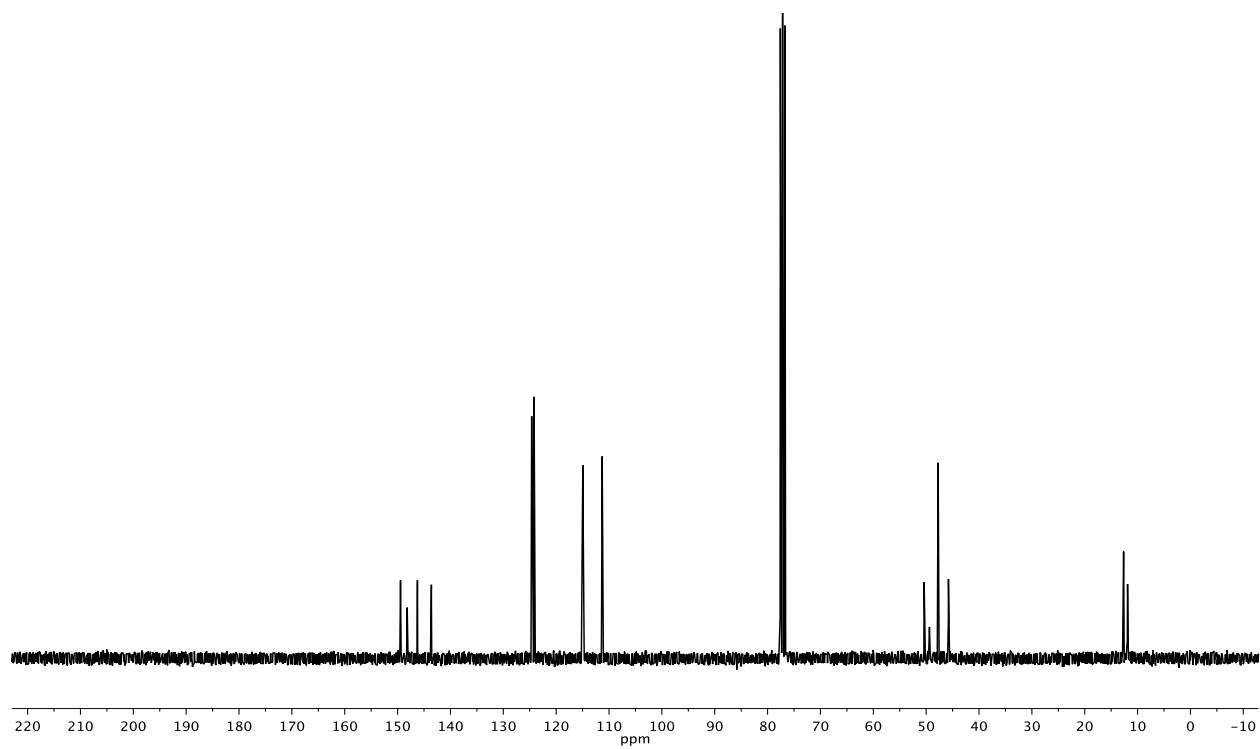
^{13}C NMR spectrum of compound 7



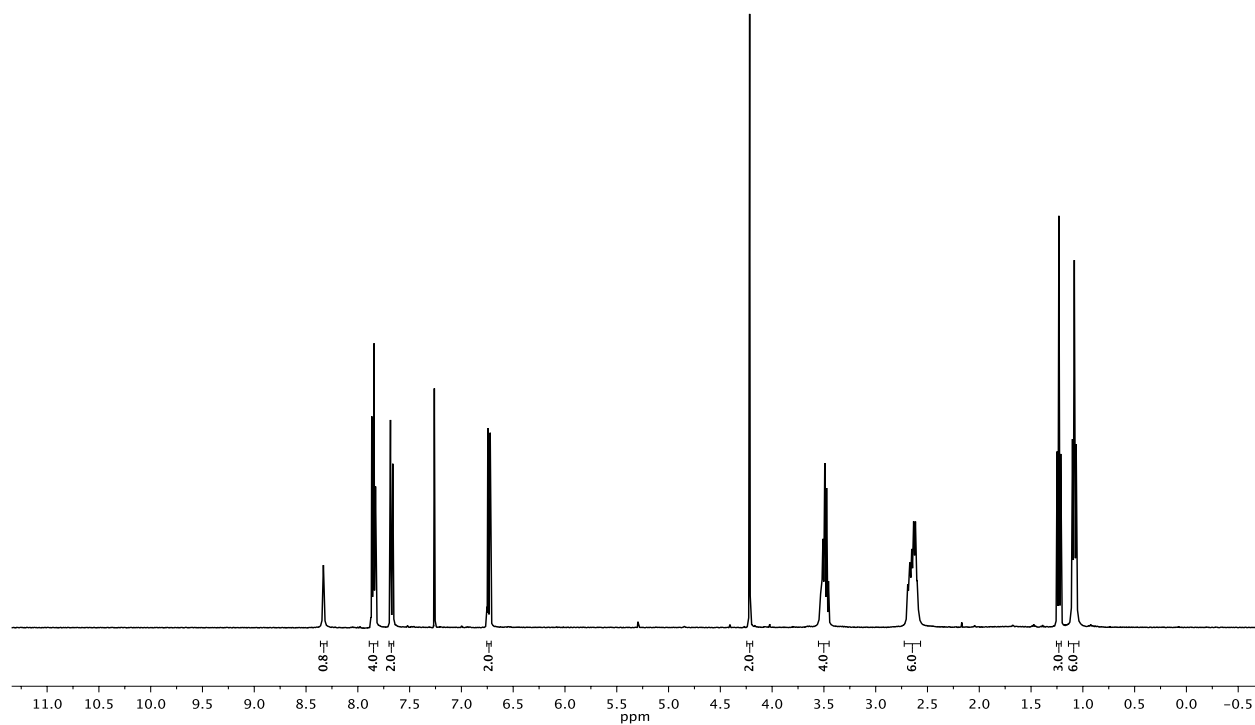
^1H NMR spectrum of compound **8**



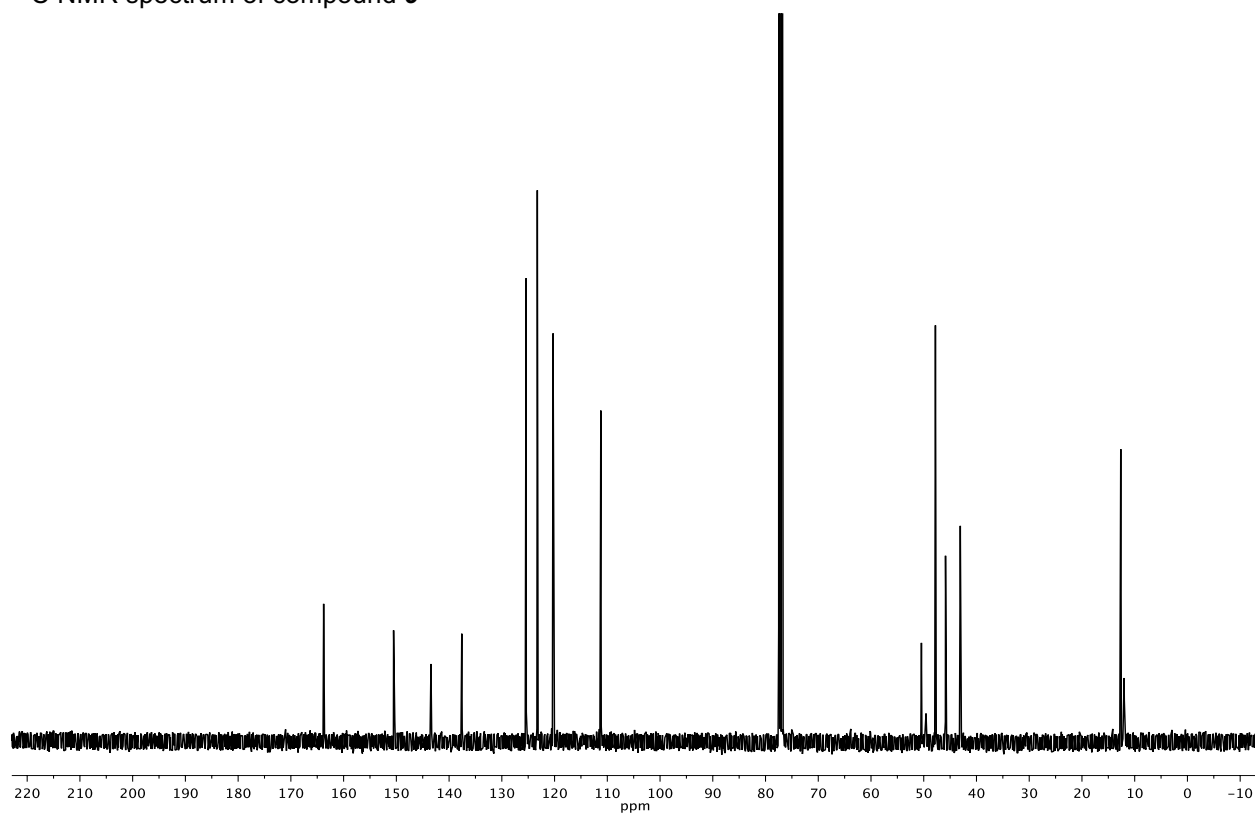
^{13}C NMR spectrum of compound **8**



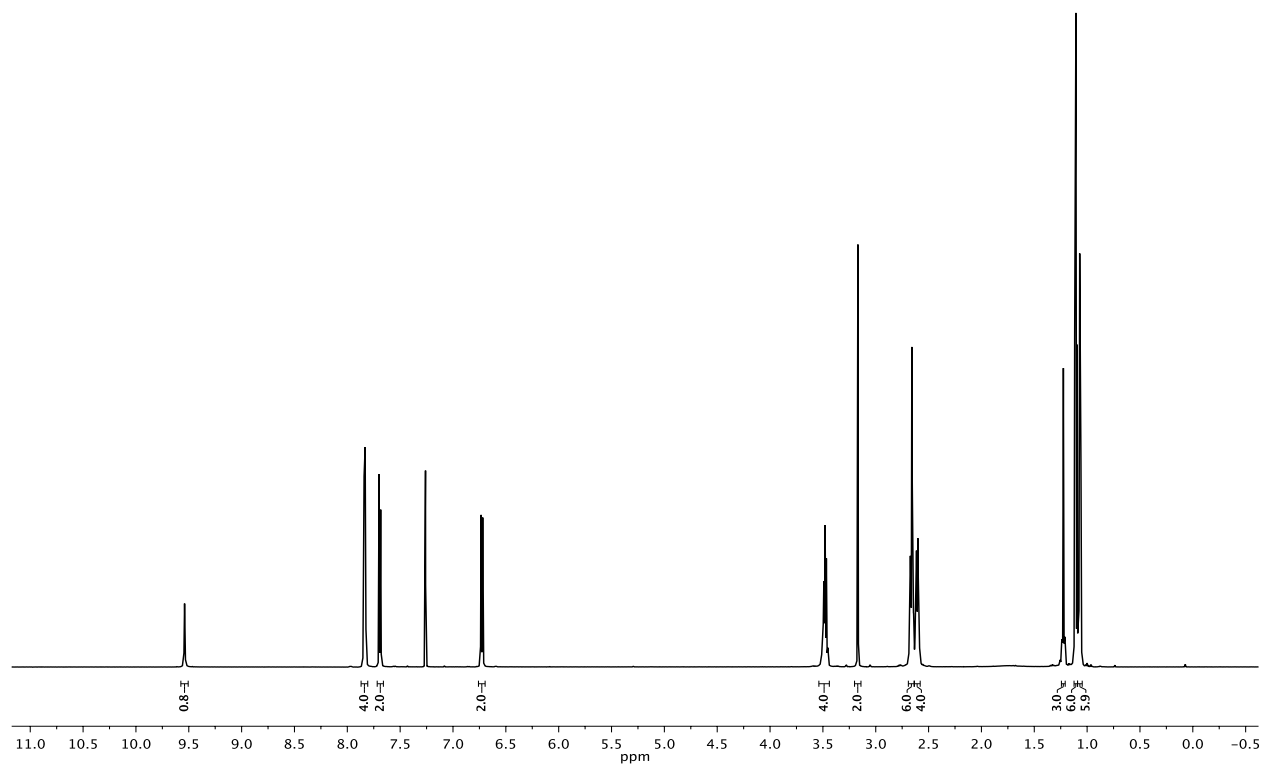
^1H NMR spectrum of compound **9**



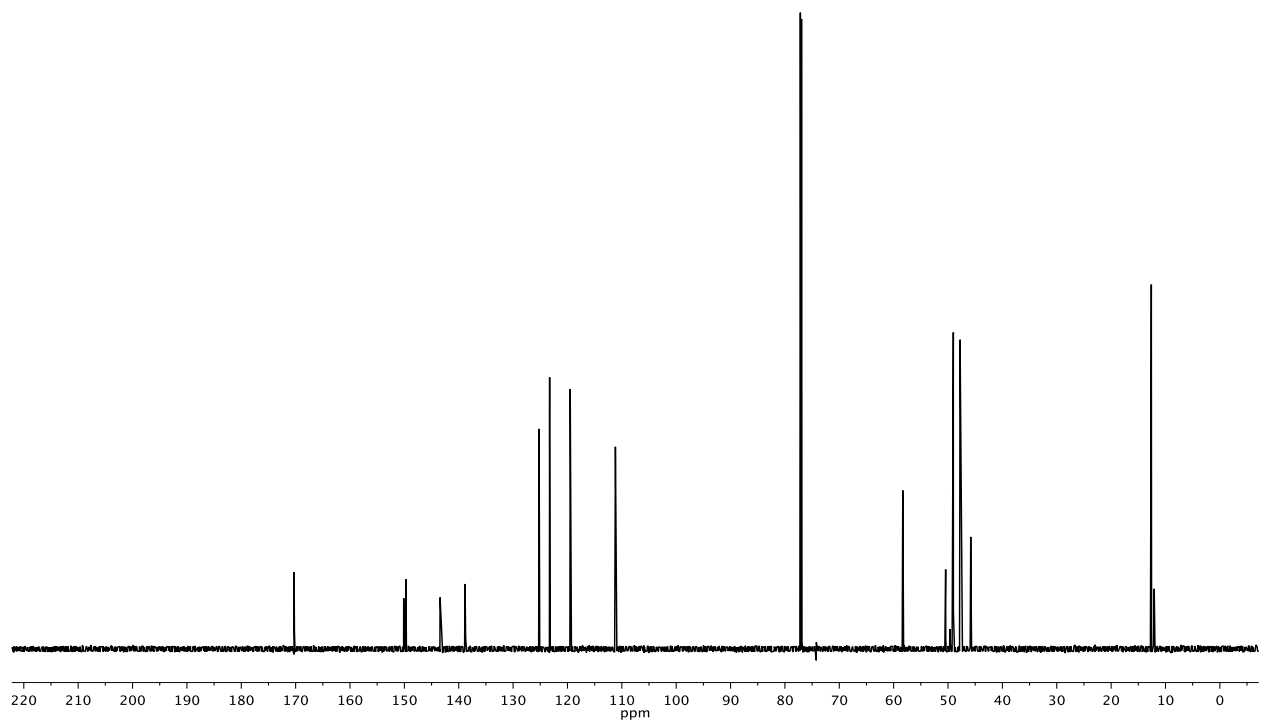
^{13}C NMR spectrum of compound **9**



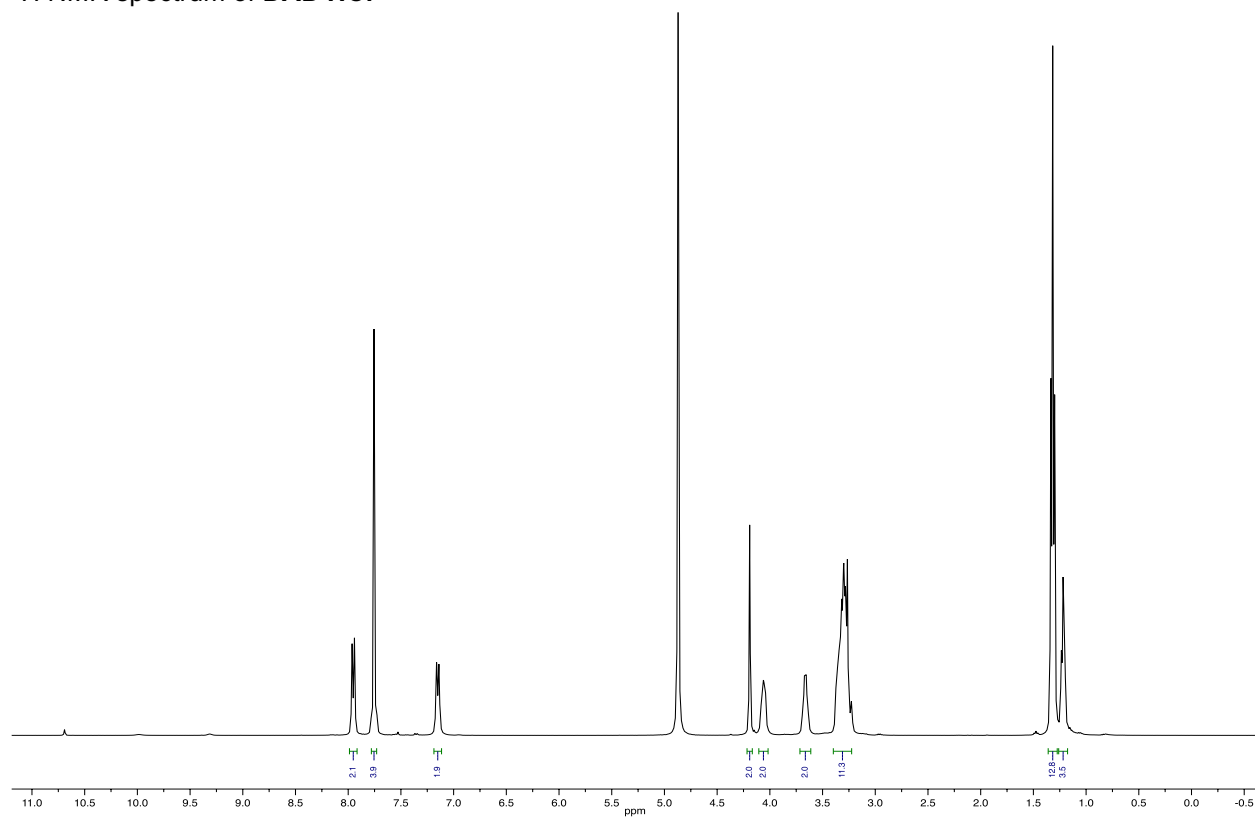
^1H NMR spectrum of **DAD (1)**



^{13}C NMR spectrum of **DAD (1)**



¹H NMR spectrum of **DAD·HCl**



¹³C NMR spectrum of **DAD·HCl**

